

1 **A quantitative tri-fluorescent yeast two-hybrid system:**
2 **from flow cytometry to *in-cellula* affinities**

3
4 **Supplementary Material**

5
6 David Cluet, Ikram Amri, Blandine Vergier, Jérémie Léault, Astrid Audibert, Clémence Grosjean,
7 Dylan Calabresi, and Martin Spichy[#]

8
9 Laboratoire de Biologie et de Modélisation de la Cellule, Ecole Normale Supérieure de Lyon,
10 CNRS, Université Lyon 1, Université de Lyon; 46 allée d'Italie; 69364 Lyon cedex 07; France.

11
12 #) corresponding author. Phone: +33 472 72 8645; Email: martin.spichy@ens-lyon.fr.

13
14 Running title: **A quantitative tri-fluorescent yeast two-hybrid system**

15

16 **Computational methods for the alchemical free energy calculations**

17 We used a standard dual topology approach where the two residues 35 and 39 of Barstar
18 were simultaneously transformed from A to D and from D to A, respectively, as a function of the
19 usual coupling parameter λ . The reader is referred to the literature for more details (1).

20 *Software*

21 Model systems were set up with the program CHARMM (2), version c39b1. Initial input
22 files for CHARMM were generated with the CHARMM-GUI server (3) and then modified to
23 implement the actual structural model with dual topology (see below). Molecular dynamics
24 simulations for free energy calculations were carried out with the program NAMD, version 2.11
25 (4).

26

27 *Model system*

28 The crystal structure of the complex Barnase:Barstar (5) served as starting point of the
29 structural model. For the alchemical transformation in Barstar alone (see left, vertical leg in Suppl.
30 Fig. S3A) only the coordinates of chain D, residues 1-89 (PDB entry 1BRS), were selected. For
31 the transformation of the complex (right vertical leg) the coordinates of Barnase (chain C, residues
32 1-110) were specified in addition to those of Barstar. Missing residue coordinates were added with
33 the help of the CHARMM-GUI server. Both systems were solvated in a cubic box (side length of
34 80 Å) of TIP3 water molecules. With the program CHARMM, residues 35 and 39 were then
35 replaced by residues with dual topology for aspartic acid (D) and alanine (A).

36

A quantitative tri-fluorescent yeast two-hybrid system

37 *Settings for molecular dynamics*

38 The systems were simulated with the CHARMM36 force field and periodic boundary
39 conditions. A cutoff of 12 Å was used for short range non-bonded interactions whereas long-range
40 electrostatic interactions were treated by Particle-Mesh Ewald (PME) with a grid spacing of 1 Å.
41 The equation of motion was integrated with a time step of 1 fs. Short range non-bonded forces were
42 updated every 2 fs, PME forces every 4 fs. The system was kept at constant pressure (1 atm) and
43 temperature (298.15 K) with a piston oscillation period of 100 fs and a damping time scale of 100
44 fs. With these MD settings the average box size of both systems (Barstar alone and complexed with
45 Barnase H102A) was almost identical (77.77 ± 0.05 vs. 77.64 ± 0.05 Å) in the following free energy
46 calculations. For systems with identical (cubic) box sizes and no change in net charge (during the
47 alchemical transformation), finite-size effects should largely cancel when comparing the two legs
48 of the alchemical transformations (6–8).

49

50 *Alchemical transformations*

51 The electrostatic interactions of the outgoing residues (here A35, D39) are linearly removed
52 from $\lambda=0$ to $\lambda=0.5$ and those of the incoming residues (D35, A39) linearly added from $\lambda=0.5$ to
53 $\lambda=1$ (NAMD parameter `alchElecLambdaStart=0.5`). The van-der-Waals interactions are scaled
54 down from $\lambda=0$ to $\lambda=1$ for the outgoing residues, and scaled up from $\lambda=0$ to $\lambda=1$ for the incoming
55 residues (`alchVdWLambdaEnd=1`). To avoid endpoint problems, we used NAMD's soft-core
56 potentials with a shifting coefficient of 4 Å. Non-bonded interactions within outgoing and incoming
57 atoms were also scaled with λ to account for interactions between residues 35 and 39
58 (`alchDecouple=off`). The actual transformation was done with a windowing method where the
59 dimer and tetramer systems were sampled by molecular-dynamics at 21 equally-separated λ -values

A quantitative tri-fluorescent yeast two-hybrid system

60 (from 0 to 1 with an increment parameter of 0.05). For each window we performed two separate
61 MD simulations. Using NAMD's FEP option, we recorded on-the-fly every 1000 fs the work
62 required to switch instantaneously the Hamiltonian from the actual window to one of the
63 neighboring windows. For the endpoints at $\lambda=0$ and 1 we performed only one MD simulation
64 (because there is only a single neighbor).

65 The free energy difference between two neighboring windows was calculated from the collected
66 work data for forward and reverse switches using Bennett's acceptance ratio (BAR) method (9).

67 The total free energy change for the transformation of λ from 0 to 1, ($= \Delta G_{\text{alchemical}}$, see also Suppl.
68 Fig. S8A) was obtained by summing up all differences between neighboring windows. After an
69 equilibration phase of 1 ns (Barstar alone) and 5 ns (complex), we monitored for blocks of 250 ps
70 (Barstar) and 1 ns (complex) the value of $\Delta G_{\text{alchemical}}$ (Suppl. Fig. S8B). The value of $\Delta G_{\text{alchemical}}$
71 fluctuates around a mean value of -0.17 ± 0.08 kcal/mol in the case of the Barstar alone and 1.71
72 ± 0.31 kcal/mol in the case of the Barstar-Barnase complex. The errors correspond to twice the
73 standard error of the mean. Finally, the difference between the two vertical legs of the
74 thermodynamic cycle of Suppl. Fig. S3A can be calculated:

$$\Delta G_{\text{alchemical}}^{\text{Barstar}} - \Delta G_{\text{alchemical}}^{\text{complex}} = -1.88 \pm 0.32 \text{ kcal/mol}$$

75 Eq. S1

76 The usual error propagation rule was used for this subtraction.

77

A quantitative tri-fluorescent yeast two-hybrid system

78 Suppl. Table S1: Primers list.

Coding Sequence	Target plasmid	Orientation	Primer name	Sequence
New expression K7 with Barstar WT	pEG-202	Forward	primSB_0001	GTGGGGTTATTGCAACGGCGACT
		Reverse	primSB_0002	GAATTCGCCCGGAATTAGCTTGGCT
Tag RFP from pTag_RFP-Actin	pSB_1Bait_Barstar	Forward	primSB_0003	CCTTATGATGTGCCAGATTATGCCTCTCCGAATTCATGG TGTCTAAGGGGGAAGAGCTGATT
		Reverse	primSB_0004	GACTCGTTTTTTCATCTCGAGGGCGGCCGAATTCATTA AGTTTGTGCCCGATTGTCTAGGG
CDS with bait extensions (Barstar mutants and Ras G12V C186A, CDK2)	pSB_1Bait_RFP	Forward	primSB_0018	GGGCACAACCTTAATGAATTCGGGGCGCCCTCGAG
		Reverse	primSB_0019	AGCTTGGCTGCAGTGCAGTCACT
Barnase H102A	pSB_1Bait_RFP	Forward	primSB_0169	GGGCACAACCTTAATGAATTCGGGGCGCCCTCGAG
		Reverse	primSB_0170	AGCTTGGCTGCAGTGCAGTCACTCACTACTCGAGTAT CTGATTTTGTAAAGTCTGATAAGCGTCC
CRaf RBD WT and A85K	pSB_1Bait_RFP	Forward	primSB_0169	GGGCACAACCTTAATGAATTCGGGGCGCCCTCGAG
		Reverse	primSB_0173	AGCTTGGCTGCAGTGCAGTCACTCACTACTCGAGCAGG AAATCTACTTGAAGTCTCTTCCAATC
SRC SH3	pSB_1Bait_RFP	Forward	primSB_0169	GGGCACAACCTTAATGAATTCGGGGCGCCCTCGAG
		Reverse	primSB_0171	AGCTTGGCTGCAGTGCAGTCACTCACTACTCGAGGGC GCCACGTAGTGTCTGG
BLIP1	pSB_1Bait_RFP	Forward	primSB_0169	GGGCACAACCTTAATGAATTCGGGGCGCCCTCGAG
		Reverse	primSB_0174	AGCTTGGCTGCAGTGCAGTCACTCACTACTCGAGGACT AAATCCATTGCTCTTACCTG
ARMC1 from cDNA library	pSB_1Bait_RFP	Forward	primSB_0230	GGGCACAACCTTAATGAATTCGGGGCGCCCTCGAGATGA ATTCTTCCACTTCCACCATGAGTGAAG
		Reverse	primSB_0231	AGCTTGGCTGCAGTGCAGTCACTCACTACTCGAGTCA CAATAAAATGATCTGGATAAAAAGTTTCAGC
Emerin from cDNA library	pSB_1Bait_RFP	Forward	primSB_0232	GGGCACAACCTTAATGAATTCGGGGCGCCCTCGAGATGG ACAACCTACGAGATCTTTCGRTAC
		Reverse	primSB_0233	AGCTTGGCTGCAGTGCAGTCACTCACTACTCGAGCTAG AAGGGTGTGCTTCTTCAGC
CksHs1	pSB_1Bait_RFP	Forward	primSB_0240	GGGCACAACCTTAATGAATTCGGGGCGCCCTCGAGATGG CGCACAAACAAATTTACTATTCCGCAAAATAC
		Reverse	primSB_0241	AGCTTGGCTGCAGTGCAGTCACTCACTACTCGAGTTTC TTTGTGTTCTTGGTAGTGGGG
New expression K7 with Barnase H102A	pJG4-5	Forward	primSB_0010	CCTTATGATGTGCCAGATTATGCCTCTC
		Reverse	primSB_0011	CCAAACCTCTGGCGAAGATCCAAA
yEGFP from pGY-LexA-GFP_KanMX	pSB_1Prey_Barnase H102A	Forward	primSB_0012	CCTTATGATGTGCCAGATTATGCCTCTCCGAATTCATGA CGAAGGGCGAGGAGCTGTTTC
		Reverse	primSB_0013	GTTGATAACCTGTGCTCGAGGGCGGCCGAATTCCTTG TACAGCTGTCCATGCCGAG
CDS with prey extensions (CRaf RBD WT and A85K, CksHs1)	pSB_1Prey_yEGFP	Forward	primSB_0020	GACGAGCTGTACAAGGAATTCGGGGCGCCCTCGAG
		Reverse	primSB_0021	AAGTCCAAAGCTTCCATGTCTCACTCACTTA
Barstar WT and mutants	pSB_1Prey_yEGFP	Forward	primSB_0165	GACGAGCTGTACAAGGAATTCGGGGCGCCCTCGAG
		Reverse	primSB_0164	AAGTCCAAAGCTTCCATGTCTCACTCACTACTCGAGTTAA GAAAGTATGATGGTATGTCCGAGCC
Ras G12V C186A	pSB_1Prey_yEGFP	Forward	primSB_0165	GACGAGCTGTACAAGGAATTCGGGGCGCCCTCGAG
		Reverse	primSB_0166	AAGTCCAAAGCTTCCATGTCTCACTCACTACTCGAGTCAG GAGGCACTGCTTTCAGC
Nef LAI	pSB_1Prey_yEGFP	Forward	primSB_0165	GACGAGCTGTACAAGGAATTCGGGGCGCCCTCGAG
		Reverse	primSB_0167	AAGTCCAAAGCTTCCATGTCTCACTCACTACTCGAGGCAG TCTTGAAGTACTCCGGATGC
TEM	pSB_1Prey_yEGFP	Forward	primSB_0165	GACGAGCTGTACAAGGAATTCGGGGCGCCCTCGAG
		Reverse	primSB_0168	AAGTCCAAAGCTTCCATGTCTCACTCACTACTCGAGCCAA TGCTTAATCAGTGAAGCCACTATC
ARMC1 from cDNA library	pSB_1Prey_yEGFP	Forward	primSB_0234	GACGAGCTGTACAAGGAATTCGGGGCGCCCTCGAGATGA ATTCTTCCACTTCCACCATGAGTGAAG
		Reverse	primSB_0235	AAGTCCAAAGCTTCCATGTCTCACTCACTACTCGAGTCA CAATAAAATGATCTGGATAAAAAGTTTCAGC
Emerin from cDNA library	pSB_1Prey_yEGFP	Forward	primSB_0236	GACGAGCTGTACAAGGAATTCGGGGCGCCCTCGAGATGG ACAACCTACGAGATCTTTCGRTAC
		Reverse	primSB_0237	AAGTCCAAAGCTTCCATGTCTCACTCACTACTCGAGCTAG AAGGGTGTGCTTCTTCAGC
CDK2	pSB_1Prey_yEGFP	Forward	primSB_0238	GACGAGCTGTACAAGGAATTCGGGGCGCCCTCGAGATGG AGAACCTCCAAAAGTGGAAAAGATCG
		Reverse	primSB_0239	AAGTCCAAAGCTTCCATGTCTCACTCACTACTCGAGGAT CSAAGATGGGTACTGGCTT
Gal1 promoter delta Gal4 with 8 operator LexA and the Kozack sequence with a new downstream MCS	pSH18-34	Forward	primSB_0076	GGACGCAAGGAAGTTAATAATCATATTACATGGC
		Reverse	primSB_0077	GAAAAAATATAATGACTAAATCTCATTGAGAAGAGTGG GGCGCGCGCTAGC
Gal1 Nterm sequence	pSH18-34	Forward	primSB_0078	CATTGAGAGAGTGGGGCGCCGCTAGCATTGTACTCG AGTTCAATTCTAGCGCAAAAG
		Reverse	primSB_0079	CCAAAGCTTGGCCAAGCCCGACTCGAG
Tag-BFP from pTag_BFP-Actin	pSH18-34	Forward	primSB_0084	ATTCCAAGCTTGGCCAAGCCCGACTCGAGATGAGCGAGC TGATTAAGGAGAACATGC
		Reverse	primSB_0085	CTGACAAAGCTGGGGCACAGCTTAATTAACCTCGAGTAAT AACCGGGCAGGCCATGTCTG
Gal1 terminator sequence	pSH18-34	Forward	primSB_0080	TAATCTGAGTAATAACCGGGCAGGCCATGTCTG
		Reverse	primSB_0081	TAATAAAAACGCCCTTCCCGGACG
Tag-BFP from pTag_BFP-Actin	pSB_3RO	Forward	primSB_0120	AAATCTCATTGAGAGAAGTGGGGCGCCGCTAGCATGA CGAGCTGATTAAGGAGAACATGC
		Reverse	primSB_0121	CTTTGGCTGAGATTGAATCAGGTACAATGCTAGCATT AGCTTGTGCCCGATTGTCTAGG

A quantitative tri-fluorescent yeast two-hybrid system

80 **Suppl. Table S2: Macsquant VYB settings for qY2H fluorescence acquisition.**

Channel	Setting
FSC	229V
SSC	265V
V1	264V
B1	327V
Y1	506V

81

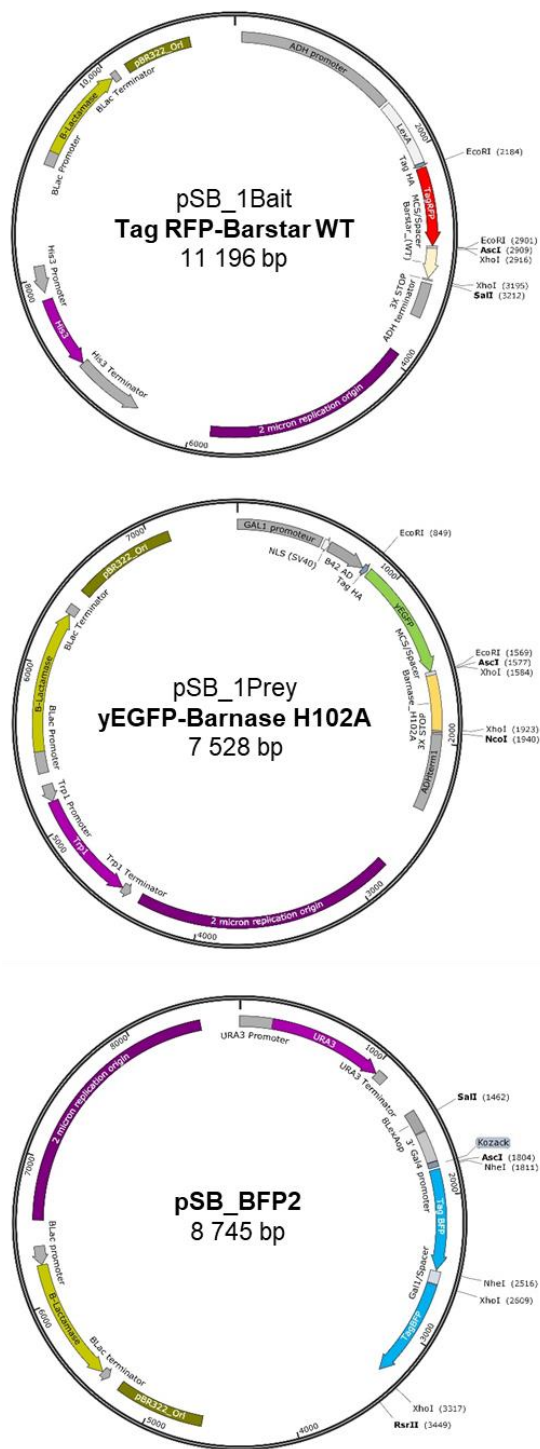
Parameter	Setting
Mixing mode	Strong
Flow speed	Medium

82

83

84

A quantitative tri-fluorescent yeast two-hybrid system



85

86 **Suppl. Fig. S1.** qY2H plasmid maps.

87

A quantitative tri-fluorescent yeast two-hybrid system

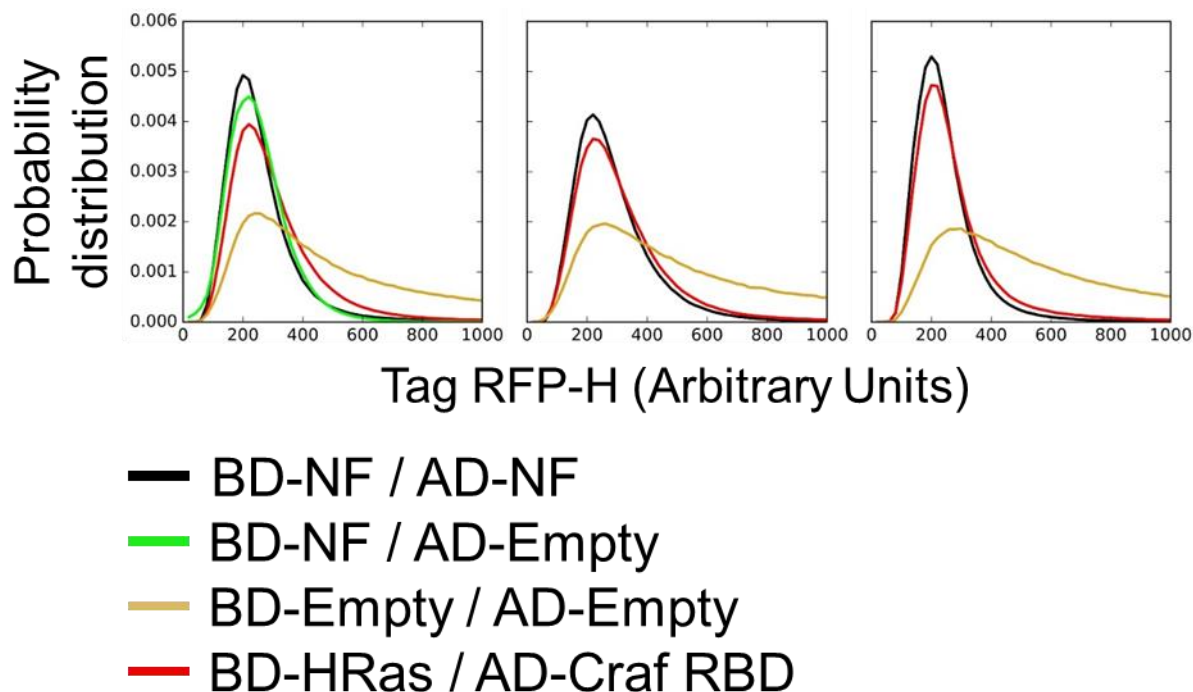
		Barstar Y29F		Barstar WT		Barstar Y29A		Barstar W38F		Barstar D35A		Barstar D39A	
		BD-Bait	AD-Prey	BD-Bait	AD-Prey	BD-Bait	AD-Prey	BD-Bait	AD-Prey	BD-Bait	AD-Prey	BD-Bait	AD-Prey
Barnase H102A	BD-Bait		[[4.496]]		[[4.28]]		[[4.81]]		[[4.30]]		[[1.04]]		[[0.87]]
	AD-Prey	[[13.45]]		[[12.10]]		[[10.62]]		[[8.43]]		[[2.06]]		[[1.52]]	
		FstI3											
		BD-Bait		BD-Bait		BD-Bait		BD-Bait		BD-Bait		BD-Bait	
Myosatin	BD-Bait												
	AD-Prey												
		CRaf RBD		CRaf RBD A85K									
		BD-Bait	AD-Prey	BD-Bait	AD-Prey	BD-Bait	AD-Prey	BD-Bait	AD-Prey	BD-Bait	AD-Prey	BD-Bait	AD-Prey
HRas G12V	BD-Bait		[[1.80]]		[[6.23]]								
	AD-Prey												
		CDK2											
		BD-Bait	AD-Prey	BD-Bait	AD-Prey	BD-Bait	AD-Prey	BD-Bait	AD-Prey	BD-Bait	AD-Prey	BD-Bait	AD-Prey
CksHs1	BD-Bait		[[2.34]]										
	AD-Prey	[[1.46]]											
		SRC SH3											
		BD-Bait	AD-Prey	BD-Bait	AD-Prey	BD-Bait	AD-Prey	BD-Bait	AD-Prey	BD-Bait	AD-Prey	BD-Bait	AD-Prey
Nef LAI	BD-Bait		[[1.19]]										
	AD-Prey												
		BLIP1											
		BD-Bait	AD-Prey	BD-Bait	AD-Prey	BD-Bait	AD-Prey	BD-Bait	AD-Prey	BD-Bait	AD-Prey	BD-Bait	AD-Prey
TEM	BD-Bait		[[1.48]]										
	AD-Prey	[[1.35]]											
		Pex3p		Pex3p W104A									
		BD-Bait	AD-Prey	BD-Bait	AD-Prey	BD-Bait	AD-Prey	BD-Bait	AD-Prey	BD-Bait	AD-Prey	BD-Bait	AD-Prey
Pex19p	BD-Bait												
	AD-Prey												
		Vav1											
		BD-Bait	AD-Prey	BD-Bait	AD-Prey	BD-Bait	AD-Prey	BD-Bait	AD-Prey	BD-Bait	AD-Prey	BD-Bait	AD-Prey
Grb2	BD-Bait		[[1.02]]										
	AD-Prey	[[1.00]]											
		Emerin											
		BD-Bait	AD-Prey	BD-Bait	AD-Prey	BD-Bait	AD-Prey	BD-Bait	AD-Prey	BD-Bait	AD-Prey	BD-Bait	AD-Prey
ARMC1	BD-Bait		[[2.05]]										
	AD-Prey	[[1.11]]											
		MNAT1											
		BD-Bait	AD-Prey	BD-Bait	AD-Prey	BD-Bait	AD-Prey	BD-Bait	AD-Prey	BD-Bait	AD-Prey	BD-Bait	AD-Prey
GMPPA	BD-Bait		[[0.92]]										
	AD-Prey	[[2.31]]											

88 **Suppl. Fig. S2.**

89 **Determination of the optimal orientation for PPI couples of Table 1.** Since certain proteins
90 showed a significant auto-activation level when used as BD-Bait fusion (see Table 2), some of the
91 orientations could not be tested (red-colored fields). For the remaining orientations, we determined
92 $\langle \text{Tag BFP-H} \rangle_{\text{sample}} / \langle \text{Tag BFP-H} \rangle_{\text{CTRL}}$, *i.e.*, the mean reporter level of a given sample relative to
93 BD-Empty / AD-Empty control sample; the relative reporter level was calculated either for the
94 entire population of cells or for a double-gated subpopulation (indicated by [[...]], see
95 “Experimental Procedures”, subsection “Data analyses”). When an orientation gave a relative
96 reporter level larger than two times the relative standard deviation of the BD-Empty / AD-Empty
97 control (0.19), it is represented in blue. If both orientations fulfill this criterion; the orientation with
98 the larger reporter level is indicated in dark blue.

99

A quantitative tri-fluorescent yeast two-hybrid system



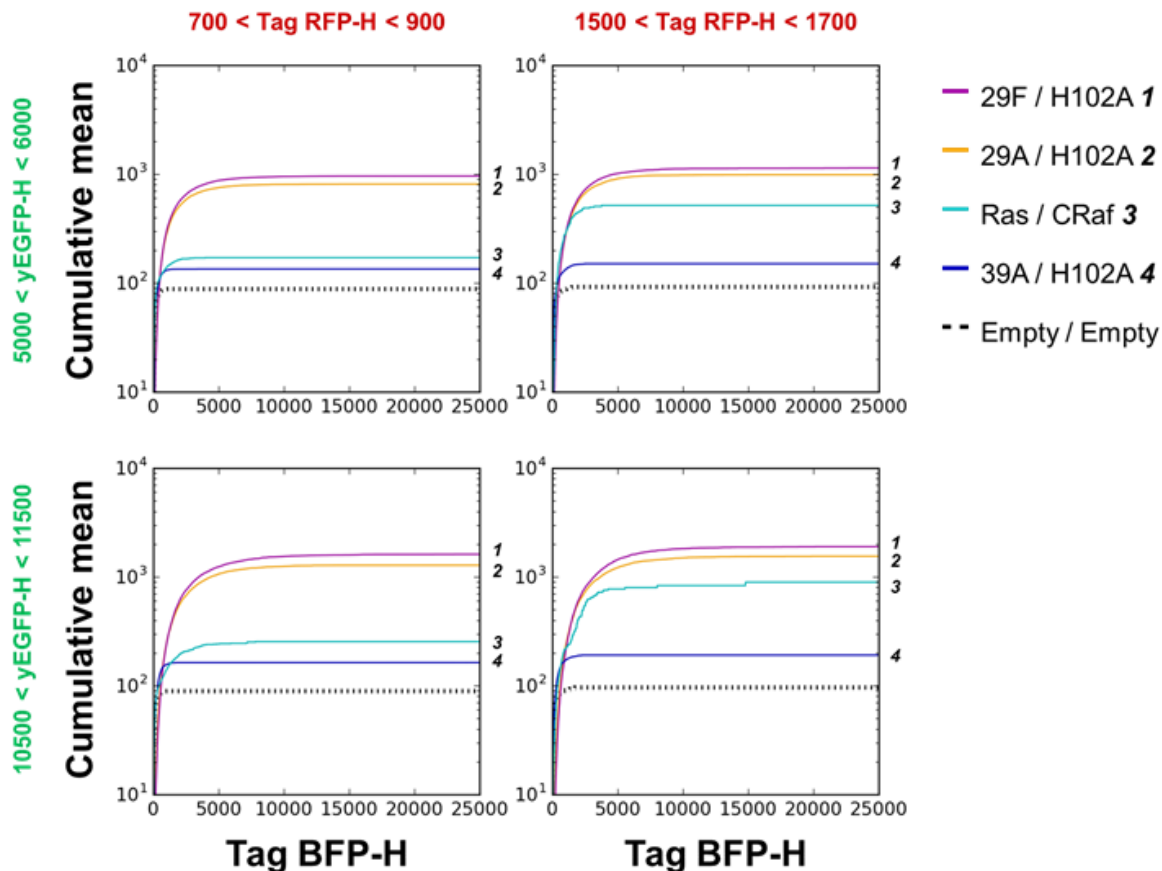
100

101 **Suppl. Fig. S3.**

102 **Detection of BD-HRas expression by flow-cytometry.** BD-HRas is not detectable by western
103 blot (see Fig. 3). But a weak expression level can be observed by flow-cytometry. The linear Tag-
104 RFP-H signals were represented as probability distributions for the BD-HRas / AD-CRAF couple
105 (Red). The non-fluorescent control, BD-NF / AD-NF, is presented in Black. In order to detect
106 compensation issues between the yEGFP and Tag-RFP channels we added the BD-NF / AD-Empty
107 couple that displays the strongest yEGFP-H signals. In our acquisition conditions the two negative
108 controls have comparable distributions, when BD-HRas generates a weak but reproducible increase
109 in the distribution (three independent experiments are presented). For comparison the BD-Empty /
110 AD-Empty couple (orange), with an optimal Bait expression level is displayed.

111

112



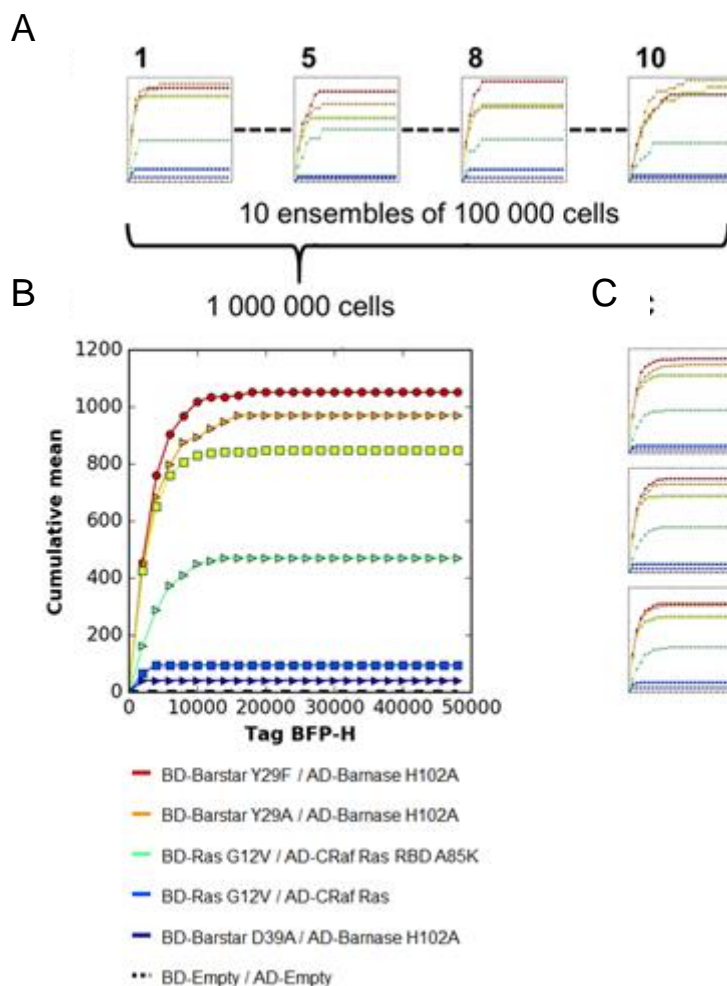
113

114 **Suppl. Fig. S4.**

115 **Impact of the gating region on the qY2H affinity ladder.** The same double gating approach as
 116 in Fig. 4 was used with two different intervals for each channel: 700-900 and 1500-1700 for Tag
 117 RFP-H, and 5000-6000 and 10500-11500 for yEGFP-H, respectively. The four different
 118 combinations do not affect the ordering of the couples. Only their relative positions vary from one
 119 gates combination to another. The analysis was performed with samples of ten millions cells.

120

121



122

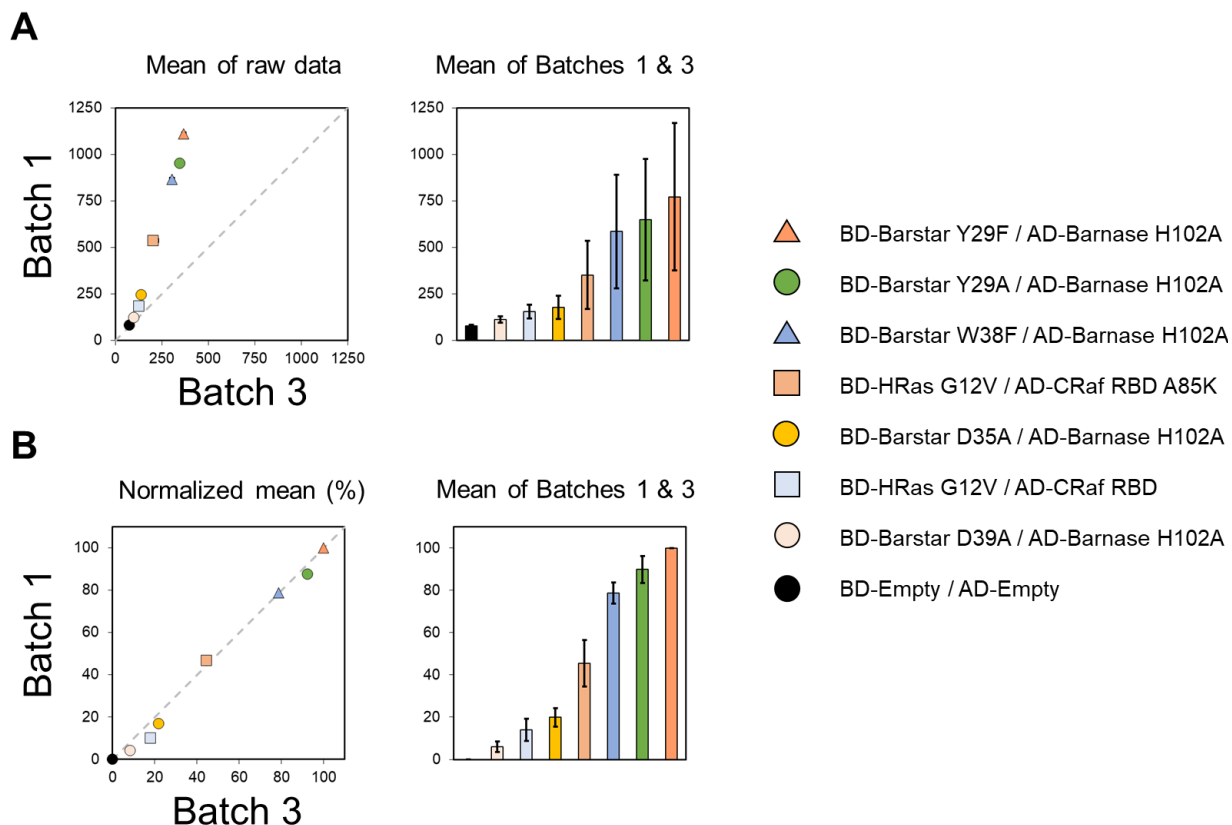
123 **Suppl. Fig. S5.**

124 **Impact of the number of cells on the qY2H affinity ladder.** A. Ten successive sub-ensembles of
 125 100 000 cells from one single experiment were used to perform a qY2H affinity ladder analysis.
 126 Background signal (BD-Empty / AD-Empty) was removed for all samples. Some sub-ensembles
 127 (*e.g.*, **5**) lead to a correct order of the PPIs according to their affinities, but several sub-ensembles
 128 gave wrong results (**1**, **8**, **10**). B. When the ten sub-ensembles were combined to a single ensemble
 129 of one million cells, a correct affinity ladder was obtained. C. The affinity ladders obtained from
 130 three subsequent ensembles of one million cells are presented. They all show the same correct order
 131 as in Fig. 4.

132

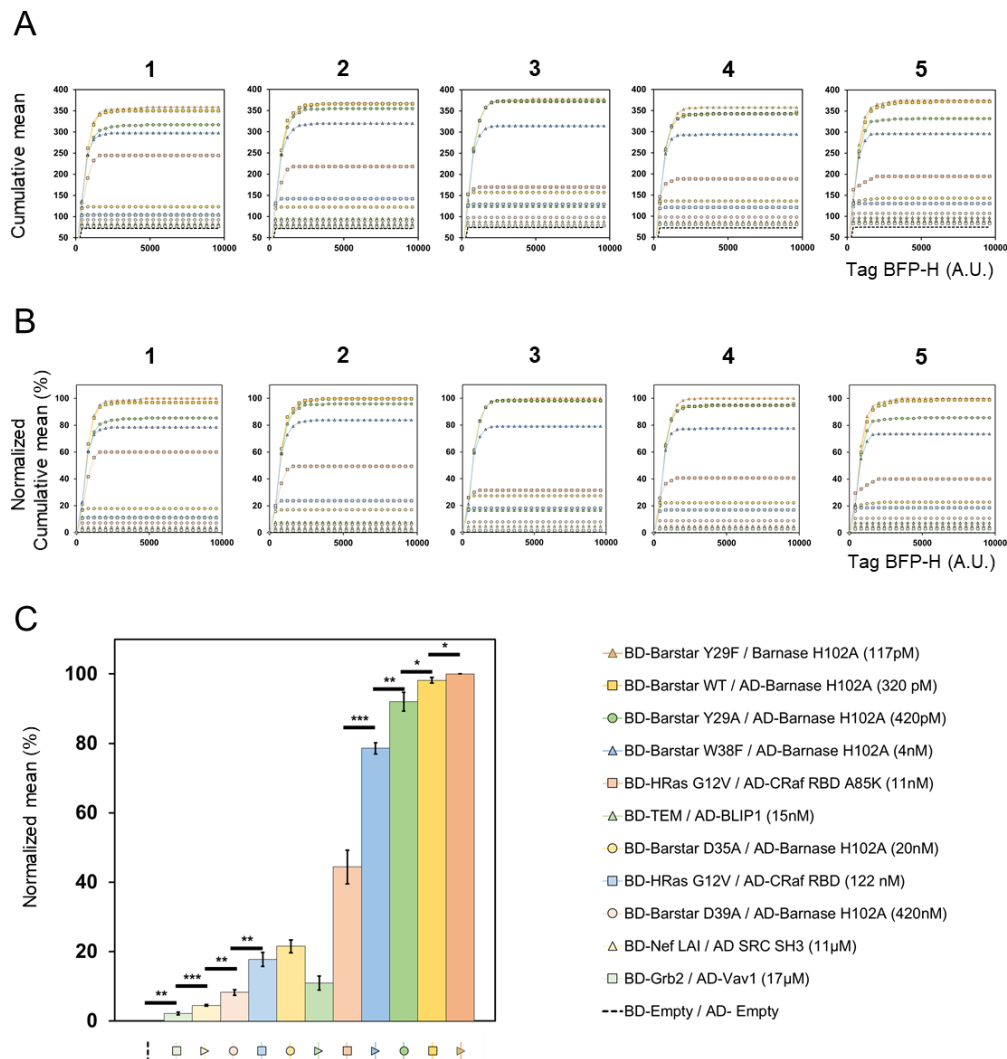
133

A quantitative tri-fluorescent yeast two-hybrid system



134 **Suppl. Fig. S6**
 135 **Reporter level for different batches of chemo-competent Yeasts.** Several repetitions of the
 136 qY2H experiments were performed with two different batches of competent yeasts (1 and 3 of
 137 Supp. Data 1). The reporter level <TagBFP-H> of seven different couples of Table 1 was
 138 determined for each repetition by analyzing one million cells. For each couple, the average of
 139 <TagBFP-H> was calculated for the five and six repetitions originating from batch 1 and 3,
 140 respectively. **A.** The correlation of the averages between batches 1 and 3 is shown for the raw data
 141 on the left side. The curve corresponding to a perfect correlation is presented as a dashed line. The
 142 quasi-linear correlation for the seven different couples implies that a similar scaling factor applies
 143 to all repetitions originating from the same batch of yeasts. When combining Batches 1 & 3, the
 144 mean values and sample standard deviations on the right side are obtained. **B.** Once the reporter
 145 levels are normalized (as explained in “Experimental procedures”, subsection “Statistical
 146 analyses”), the scaling factor is largely attenuated (left side) and the (absolute and relative) sample
 147 standard deviations are reduced significantly for most couples with respect to the raw data (right
 148 side).

A quantitative tri-fluorescent yeast two-hybrid system

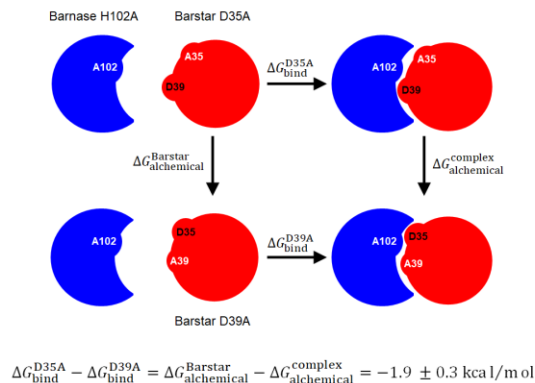


149 **Suppl. Fig. S7**

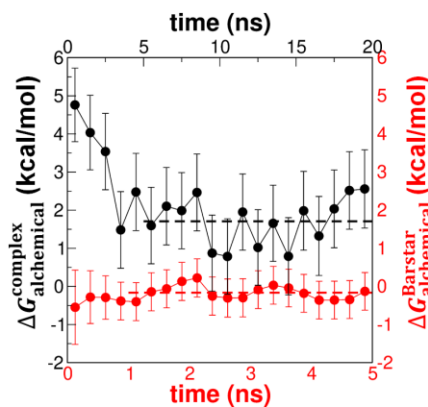
150 **Reproducibility of the affinity ladder and its normalization.** Five repetitions of the qY2H
 151 experiment were performed with the same batch of competent yeasts. For all samples, one million
 152 of cells were analyzed; the same gates as in Fig. 5 (main text) were applied. *A.* The plotting of the
 153 cumulative means (with raw data) for each repetition yielded five similar affinity ladders where the
 154 couples are ordered according to their affinity (Table 1). An exception is the couple BD-TEM /
 155 AD-BLIP1 that is ranked too low in all repetitions. Also, the couple BD-HRas G12V / AD-CRaf
 156 is ranked too high in experiment 2. Note that in experiment 4, no yeast cells were detected for BD-
 157 TEM / AD-BLIP1 in the double gated region. *B.* Affinity ladders are shown for normalized
 158 cumulative means. First, the cumulative mean of the BD-Empty / AD-Empty control sample (*i.e.*,
 159 background of the qY2H system) is removed from the cumulative mean of all samples. Second,
 160 the background-corrected cumulative means are normalized with the corresponding value of the
 161 couple BD-Barstar Y29F / AD-Barnase H102A ($K_d=117$ pM). *C.* The normalized means were
 162 used to calculate the average value of the five repetitions. Error bars correspond to the standard
 163 error of the mean. The statistical significance of the difference between direct neighbors of the
 164 ladder is indicated (* : p-value < 0.05, ** : p-value < 0.01, *** : p-value < 0.001).

A quantitative tri-fluorescent yeast two-hybrid system

A



B

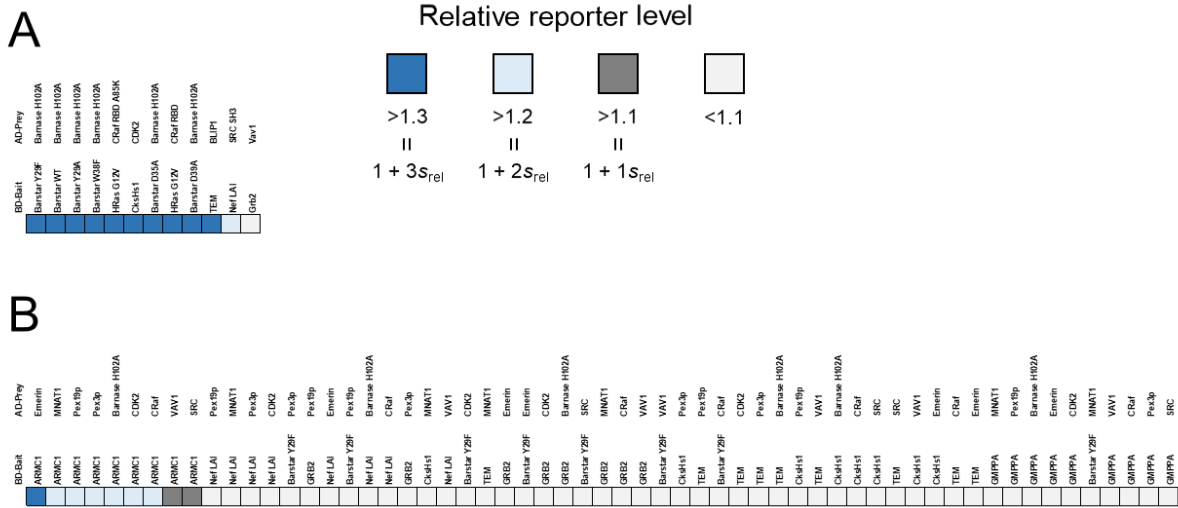


165

166 **Suppl. Fig. S8.**

167 **Alchemical free energy calculations.** A. A thermodynamic cycle is applied to calculate the
 168 difference in binding free energy for the interaction between Barnase H102A and the mutants
 169 Barstar D35A (horizontal leg, top) and D39A (horizontal leg, bottom). Because the free energy is
 170 a state function, this difference can also be obtained from the free energy difference of the
 171 corresponding alchemical transformation in Barstar alone (vertical leg, left) and the complex
 172 (vertical leg, right leg). B. In the block analysis the change in free energy for the alchemical
 173 transformations is plotted for consecutive blocks of 250 ps (Barstar alone, red dots) and 1 ns
 174 (complex, black dots) of sampling. The error bars correspond to the analytical error of the
 175 maximum likelihood estimate (10). The mean value of $\Delta G_{\text{alchemical}}$ for each alchemical
 176 transformation is indicated as horizontal dashed line.

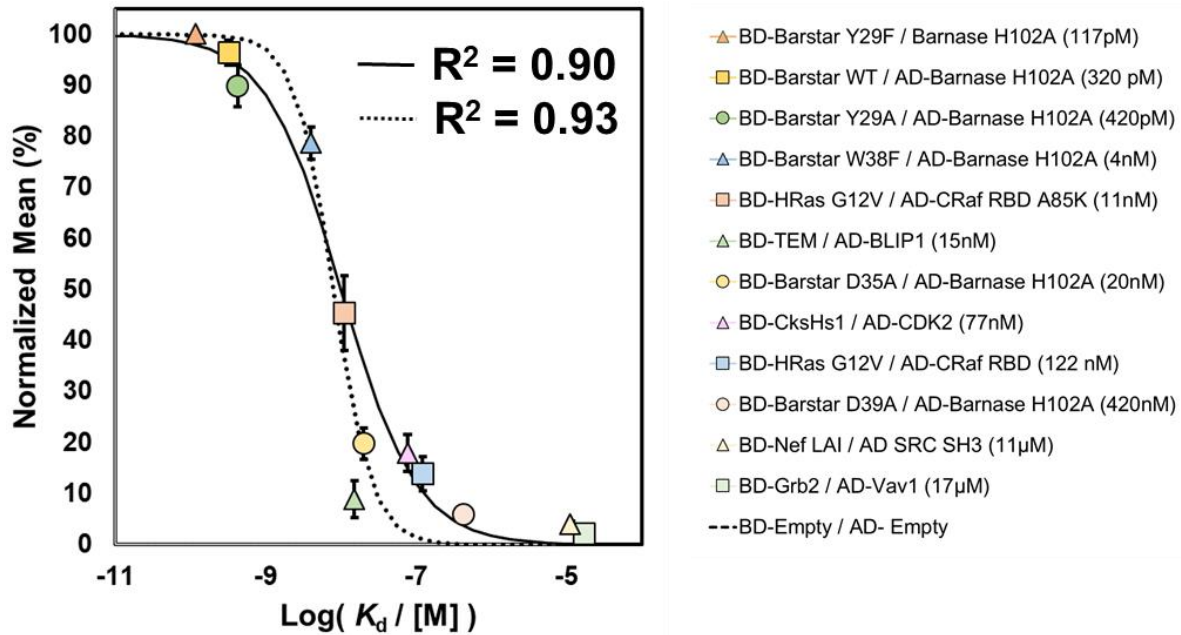
A quantitative tri-fluorescent yeast two-hybrid system



177 **Suppl. Fig. S9.**
 178 **Determination of the sensitivity and specificity of the qY2H.** We determined $\langle \text{Tag BFP-H} \rangle_{\text{sample}} / \langle \text{Tag BFP-H} \rangle_{\text{CTRL}}$, *i.e.*, the mean reporter level of a given sample relative to BD-
 179 H>sample / <Tag BFP-H>CTRL, *i.e.*, the mean reporter level of a given sample relative to BD-
 180 Empty / AD-Empty control sample; the relative reporter level was calculated for a double-gated
 181 subpopulation (see “Experimental Procedures”, subsection “Data analyses”). When a couple gave
 182 a relative reporter above the margin of error of 0.19 ($= 2 s_{rel}$, *i.e.*, two times the relative sample
 183 standard deviation of the CTRL sample BD-Empty / AD-Empty), it is represented in blue. **A.** The
 184 subfigure presents the results obtained for twelve interactions of known affinity (Table 1). Since
 185 Pex3p and Pex19p proteins showed both a significant auto-activation level when used as BD-Bait
 186 fusion (see Table 2), the two couples Pex3p WT / Pex19p and Pex3p W104A could not be tested.
 187 The couples are ranked according to their relative reporter level. Except for the BD-Grb2 / AD-
 188 Vav1 couple, all interactions generate a reporter level that can be distinguished from the
 189 background of the system. **B.** The same analysis was performed with the couples of the Specificity
 190 Test Set. Out of the 57 couples, seven are above the margin of error, one even above $3 s_{rel}$. These
 191 seven couples have the same BD-Bait fusion (BD-ARMC1) in common. The 52 other couples
 192 (91% of this set) display a relative reporter level within $1 s_{rel}$ of the CTRL sample, and cannot be
 193 distinguished from the system’s background.

194

195



196 **Suppl. Fig. S10.**

197 **Correlation between *in-vitro* measured K_d -values and the normalized mean of the qY2H**
 198 **reporter level.** Correlation between *in-vitro* measured K_d -values and the normalized mean of the
 199 qY2H reporter level. The relationship follows a classical dose-response curve that can be well fitted
 200 with a sigmoid-like generalized logistic function (Richard's curve):

$$\text{Normalized Mean (NM)} = \frac{100}{1 + e^{\alpha (\log(K_d/[M]) + \beta)}}$$

201 Eq. S2

202 with α and β two parameters to be fitted, and log the common logarithm with basis 10. When all
 203 data points (except BD-Barstar D35A / AD-Barnase H102A) are used for the least-square fitting
 204 we obtain $\alpha = 3.9$ and $\beta = 8.1$ (dashed curve). Eliminating the outlier BD-TEML / AD-BLIP1,
 205 yields $\alpha = 2.0$ and $\beta = 8.0$ (solid curve). Adjusted R^2 values (see section "Statistical analyses") were
 206 calculated for both parameter sets (with $n=12$ and $k=2$). Given the normalized reporter level, the
 207 dissociation constant can be determined with the inverse function:

$$\log(K_d/[M]) = \frac{\ln\left[\frac{100}{\text{NM}} - 1\right]}{\alpha} - \beta$$

208 Eq. S3

209 With Eq. S3 the dissociation constant of the BD-Barstar D35A / AD-Barnase H102A can be
 210 estimated to be within 18 nM ($\alpha = 3.9, \beta = 8.1$) and 49 nM ($\alpha = 2.0, \beta = 8.0$), in excellent agreement
 211 with independent free-energy calculations (20 nM).

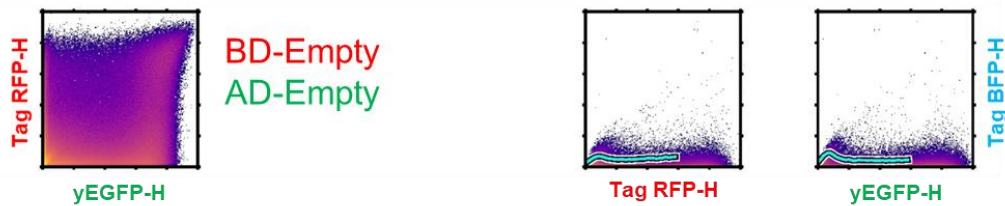
212

213 **Suppl. Data1.**

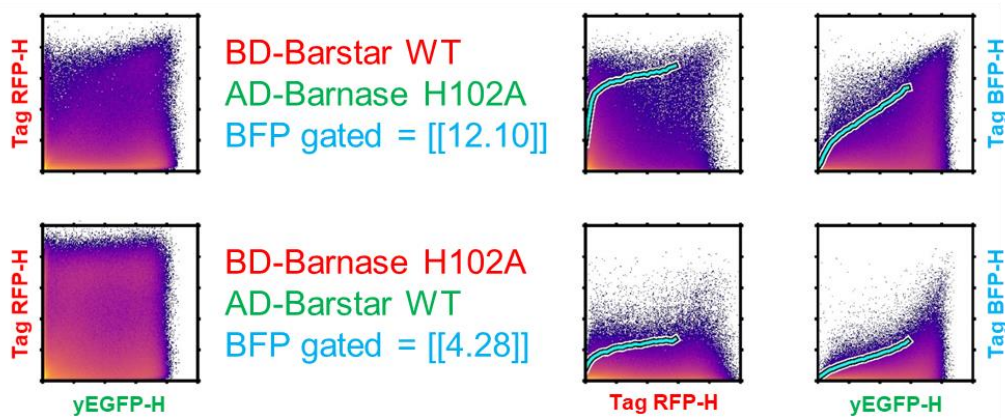
214 **Determination of the optimal orientation of each couple.** For the determination of the optimal
215 orientation for the couples of Table 1, several batches of competent EYG42A (pBFP+) competent
216 yeasts were used. For each batch, the corresponding BD-Empty / AD-Empty control is presented.
217 When possible (*i.e.* no prior detection of a significant auto-activation level) both orientation were
218 studied. One million cells were acquired for each analysis. The three channels Tag RFP-H, yEGFP-
219 H and Tag BFP-H are displayed on the hlog-scale (see “Experimental procedures”, subsection
220 “Data analyses” for the exact settings). Patterns of correlation between Tag BFP-H and Tag RFP-
221 H and between Tag-BFP-H and yEGFP-H are indicated by cyan curves. These curves were
222 obtained by discretizing the cells into 30 bins based on their TagRFP-H or yEGFP-H values. For
223 each bin the mean value of the TagBFP-H values was determined for the top 5%. In addition, the
224 relative reporter level $\langle \text{Tag BFP-H} \rangle_{\text{sample}} / \langle \text{Tag BFP-H} \rangle_{\text{CTRL}}$ for standardized expression levels
225 of BD-Bait and AD-Prey is indicated in double square brackets. Standardization is achieved by
226 applying two gates: $700 < \text{linear Tag RFP-H} < 900$ and $5000 < \text{linear yEGFP-H} < 6000$.
227

YEAST BATCH 1

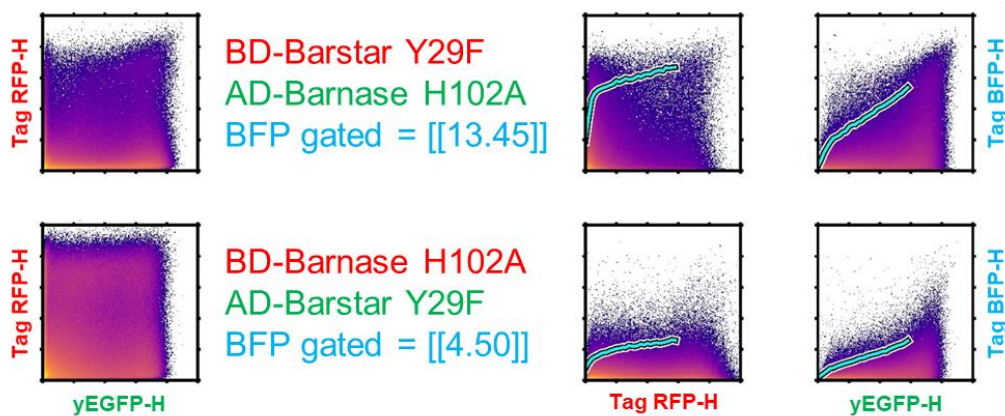
1.00 Empty / Empty



1.01 Barstar WT / Barnase H102A

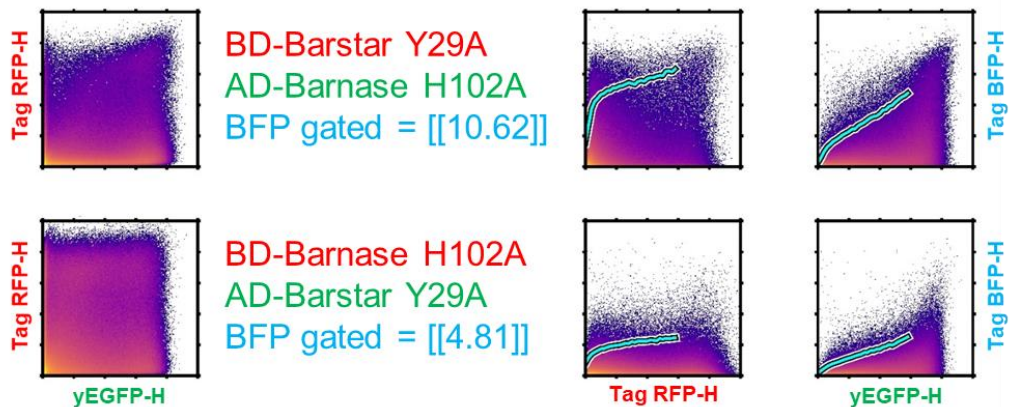


1.02 Barstar Y29F / Barnase H102A

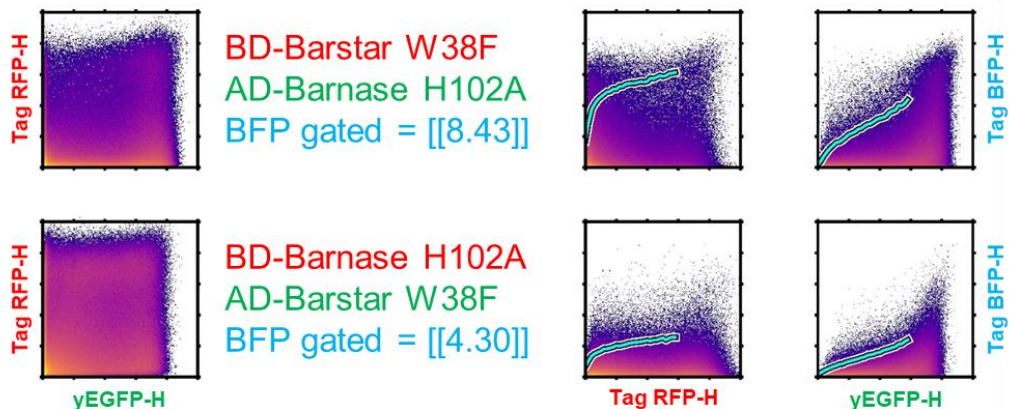


A quantitative tri-fluorescent yeast two-hybrid system

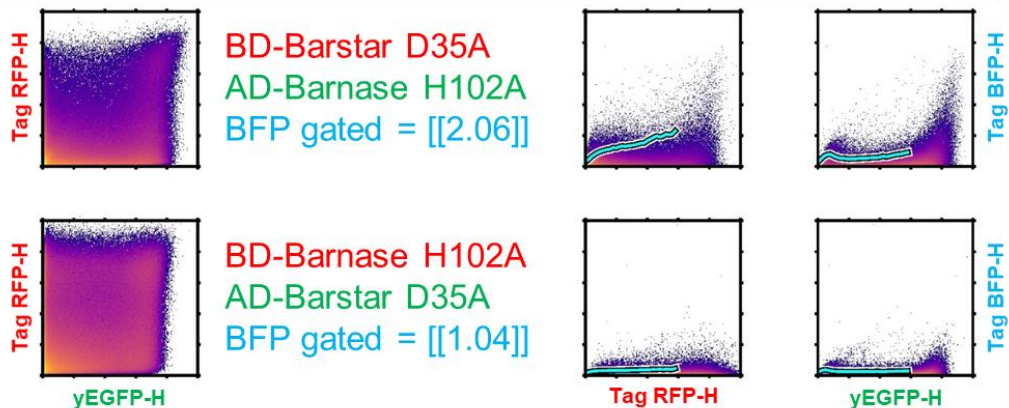
1.03 Barstar Y29A / Barnase H102A



1.04 Barstar W38F / Barnase H102A



1.05 Barstar D35A / Barnase H102A

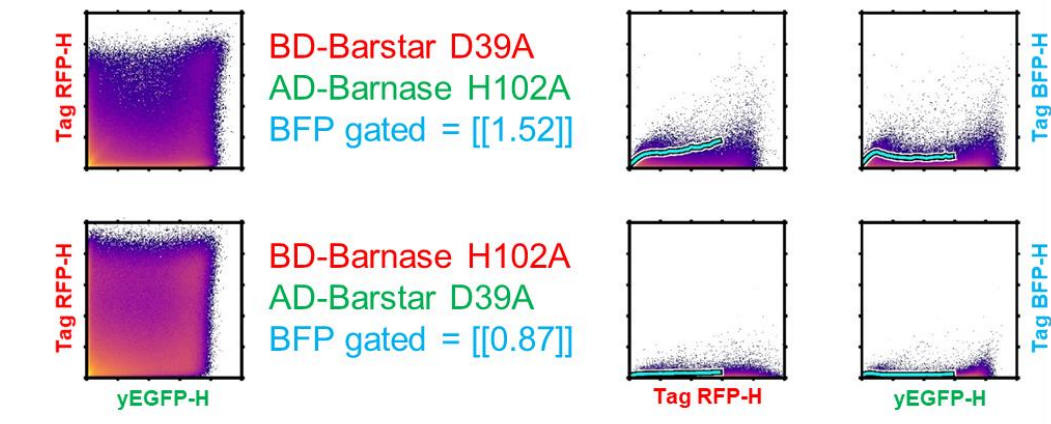


229

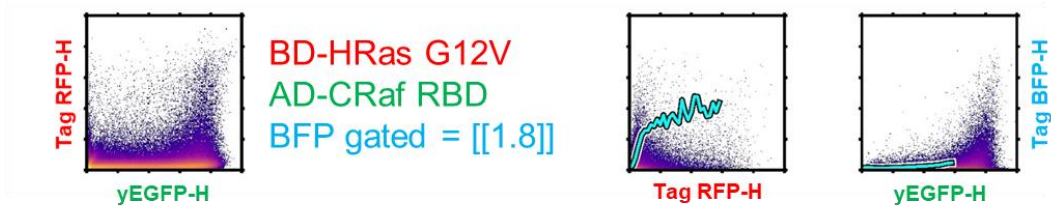
230

A quantitative tri-fluorescent yeast two-hybrid system

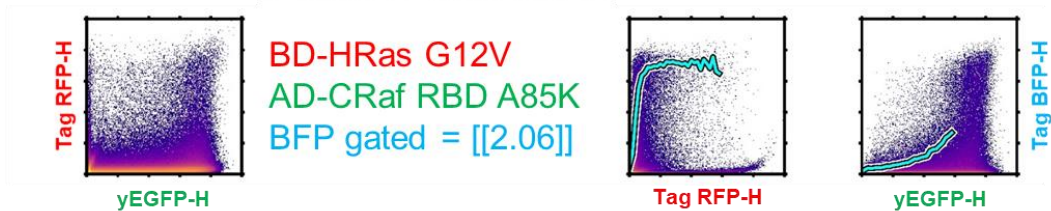
1.06 Barstar D39A / Barnase H102A



1.07 HRas G12V C186A / CRaf RBD



1.08 HRas G12V C186A / CRaf RBD A85K



231

232

233

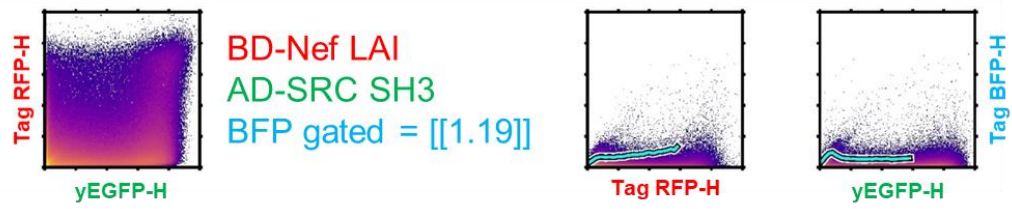
A quantitative tri-fluorescent yeast two-hybrid system

YEAST BATCH 2

2.00 Empty / Empty



2.01 Nef LAI / SRC SH3



234

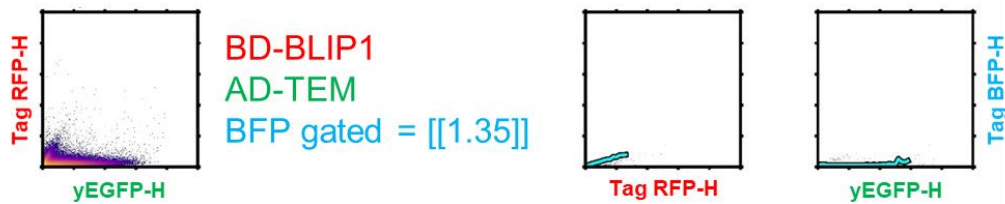
235

YEAST BATCH 3

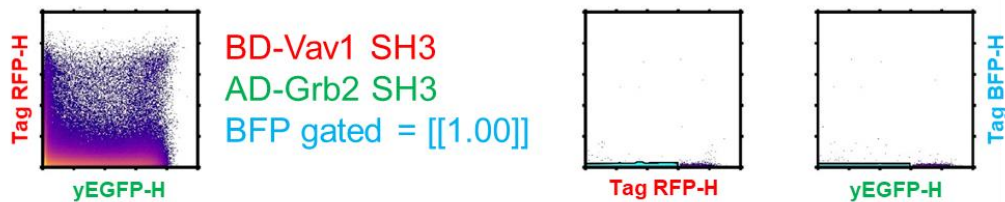
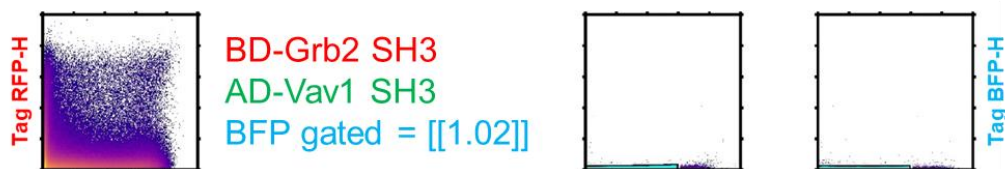
3.00 Empty / Empty



3.01 TEM / BLIP1



3.02 Grb2 SH3 / Vav1 SH3

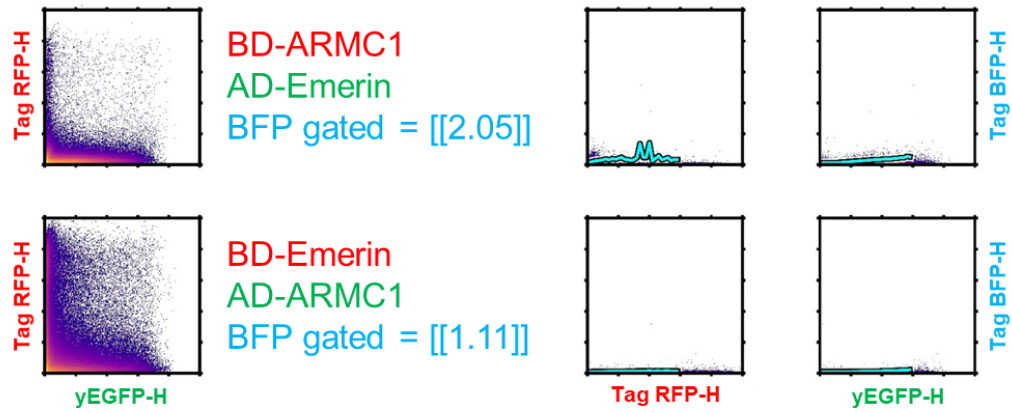


236

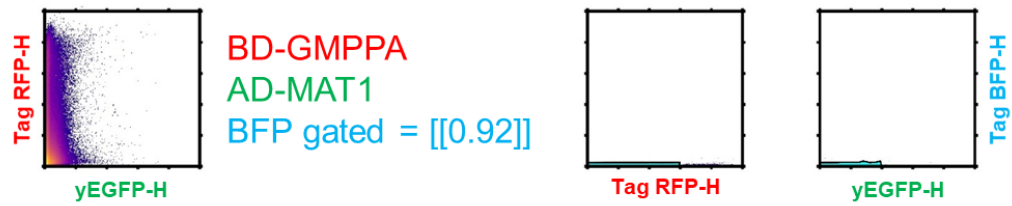
237

A quantitative tri-fluorescent yeast two-hybrid system

3.03 ARMC1 / Emerin



3.04 GMPPA / MAT1

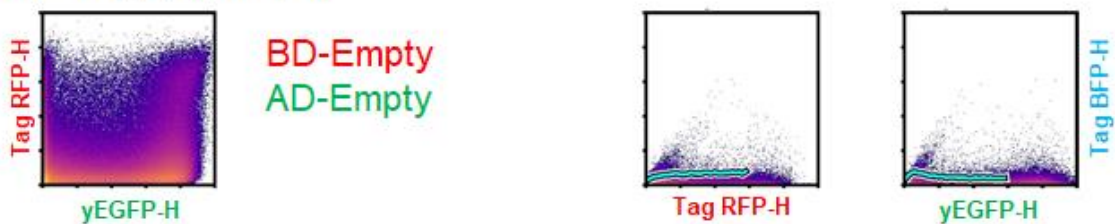


238

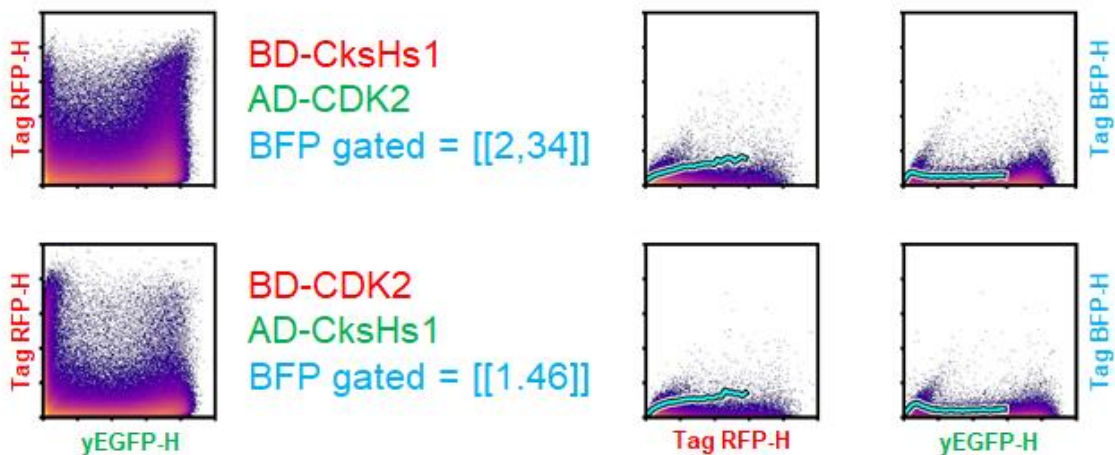
239

YEAST BATCH 4

3.00 Empty / Empty



3.01 CksHs1 / CDK2



241 **References**

- 242 1. Chipot C, Pohorille A eds. (2007) *Free energy calculations: theory and applications in*
243 *chemistry and biology* (Springer, Berlin ; New York).
- 244 2. Brooks BR, et al. (2009) CHARMM: The biomolecular simulation program. *J Comput Chem*
245 30(10):1545–1614.
- 246 3. Lee J, et al. (2016) CHARMM-GUI Input Generator for NAMD, GROMACS, AMBER,
247 OpenMM, and CHARMM/OpenMM Simulations Using the CHARMM36 Additive Force
248 Field. *J Chem Theory Comput* 12(1):405–413.
- 249 4. Phillips JC, et al. (2005) Scalable molecular dynamics with NAMD. *J Comput Chem*
250 26(16):1781–1802.
- 251 5. Buckle AM, Schreiber G, Fersht AR (1994) Protein-protein recognition: Crystal structural
252 analysis of a barnase-barstar complex at 2.0-Å resolution. *Biochemistry (Mosc)*
253 33(30):8878–8889.
- 254 6. Hummer G, Pratt LR, García AE (1996) Free Energy of Ionic Hydration. *J Phys Chem*
255 100(4):1206–1215.
- 256 7. Figueirido F, Del Buono GS, Levy RM (1997) On Finite-Size Corrections to the Free Energy
257 of Ionic Hydration. *J Phys Chem B* 101(29):5622–5623.
- 258 8. Rocklin GJ, Mobley DL, Dill KA, Hünenberger PH (2013) Calculating the binding free
259 energies of charged species based on explicit-solvent simulations employing lattice-sum

A quantitative tri-fluorescent yeast two-hybrid system

260 methods: An accurate correction scheme for electrostatic finite-size effects. *J Chem Phys*
261 139(18):184103.

262 9. Bennett CH (1976) Efficient estimation of free energy differences from Monte Carlo data. *J*
263 *Comput Phys* 22(2):245–268.

264 10. Shirts MR, Bair E, Hooker G, Pande VS (2003) Equilibrium Free Energies from
265 Nonequilibrium Measurements Using Maximum-Likelihood Methods. *Phys Rev Lett* 91(14).
266 doi:10.1103/PhysRevLett.91.140601.

267

Analysis of QY2H Data

<https://github.com/dcluet/qY2H-Affinity-Ladder>

Introduction

This program permits the automated generation of affinity ladders from quantitative Yeast Two Hybrid experiments. The program requires flow cytometry data `.fcs` files (linear scale). It generates a `.csv` table file that contains for each sample the mean reporter level. The actual affinity ladder graph is reported into a `.pdf` file. For more information, the reader is referred to our article:

A quantitative tri-fluorescent yeast two-hybrid system: from flow cytometry to in-cellula affinities

<https://www.biorxiv.org/content/10.1101/553636v1>

Authors

	  ENS DE LYON
CLUET David	david.cluet@ens-lyon.fr
SPICHTY Martin	martin.spichty@ens-lyon.fr

License

Copyright CNRS 2013

This software is a computer program whose purpose is to automatically analyze QY2H data (.fcs files) and generate *in cellulo* affinity ladder.

This software is governed by the CeCILL license under French law and abiding by the rules of distribution of free software. You can use, modify and/ or redistribute the software under the terms of the CeCILL license as circulated by CEA, CNRS and INRIA at the following URL: <http://www.cecill.info/index.en.html>

As a counterpart to the access to the source code and rights to copy, modify and redistribute granted by the license, users are provided only with a limited warranty and the software's author, the holder of the economic rights, and the successive licensors have only limited liability.

In this respect, the user's attention is drawn to the risks associated with loading, using, modifying and/or developing or reproducing the software by the user in light of its specific status of free software, that may mean that it is complicated to manipulate, and that also therefore means that it is reserved for developers and experienced professionals having in-depth computer knowledge. Users are therefore encouraged to load and test the software's suitability as regards their requirements in conditions enabling the security of their systems and/or data to be ensured and, more generally, to use and operate it in the same conditions as regards security.

The fact that you are presently reading this means that- delete the `_remote_branch` you have had knowledge of the CeCILL license and that you accept its terms.

Requirements

This program is optimized for Python 2.7 with the following libraries:

- `datetime`: To generate unique Analysis ID and file name.
- `FlowCytometryTools v 0.4.6`: To open `.fcs` files and manipulate flowcytometry data.
<http://eyurtsev.github.io/FlowCytometryTools/>
- `glob`: To identify the `.fcs` files in the Input folder.
- `matplotlib v 1.5.1`: To generate the curves.
- `numpy v 1.13.3`: To generate and manipulate arrays.
- `os`: To handle paths of the raw data and generated files.
- `Pillow / PIL v 3.1.2`: To display images within the GUI of the program.
- `sys`: To permit manual abortion of the program.
- `Tkinter v 8.6`: To generate the GUI of the program.

Files

- README.md
- LICENSE.txt
- [] **src**
 - Analysis_QY2H.py
 - [] **utils**
 - __init__.py
 - channels.config
 - Colors.py
 - Configuration.py
 - Configure_Channels.py
 - Ending_Window.py
 - Functions.py
 - Logo.jpg
 - Object_Echantillon.py
 - Opening_window.py
 - Variables.py
- [] **doc**
 - Analysis_Configuration.jpg
 - Analysis_Progress.jpg
 - Logo_cnrs.jpg
 - Logo_ens.jpg
 - Logo_LBMC.jpg
 - Logo.jpg
 - Main_Menu.jpg
 - Results.jpg
 - Select_Channels.jpg
 - Select_File.jpg
 - Select_Input.jpg
 - Select_Output.jpg

User Guide

1 Recommendation for acquisition

Our program requires linear values for all fluorescence channels. Thus, be vigilant that your acquisition program is saving data as linear (even if your acquisition display is log OR hyper log).

Yeast cells are usually smaller than the focused laser beam (spot) of flow cytometers. The maximum signal (= Height, H) for a given cell is obtained when the cell is fully covered by the laser spot. Thus, H reflects the total cellular content of the fluorophore. Therefore, we recommend to use the signal Height (H) of each channel.

Moreover, some flow-cytometers can apply internal corrections on specific channels. For example, the MacsquantVYB (that we used for our experiment) is correcting the Area A of each channels:

Area is the sum of a defined number of adjacent samples at the trigger time point divided by a scaling factor. This factor is chosen in a way that for “normal” events $H=A$ to obtain a diagonal. The scaling factor is pressure dependent.

Thus we strongly recommend to use as much as possible **non-manipulated** values.

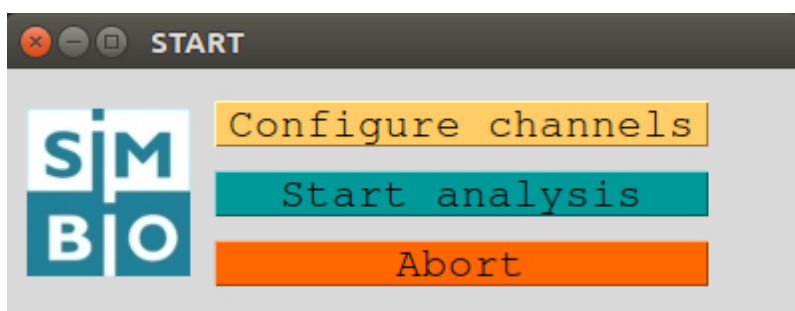
2 Main Menu

To start the program you need to execute the Analysis_QY2H.py python script:


```
$ python Analysis_QY2H.py
```

The main menu will propose you different functions:

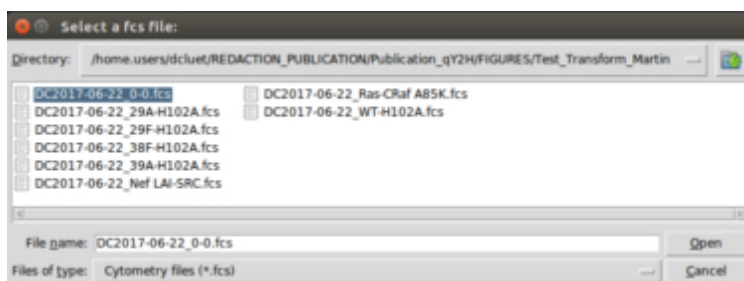
1. **Configure channels** To select the channels to be used for the analysis.
2. **Start analysis** To generate a quantitative Yeast Two Hybrid affinity ladder from a set of .fcs files.
3. **Abort** To exit the program.



3 Configure the names of the channels

Before performing your first analysis, it is recommended to configure your channels. If you keep always the same acquisition settings, this step is required only once.

When clicking on `Configure channels`, the program prompts you to choose a .fcs file.

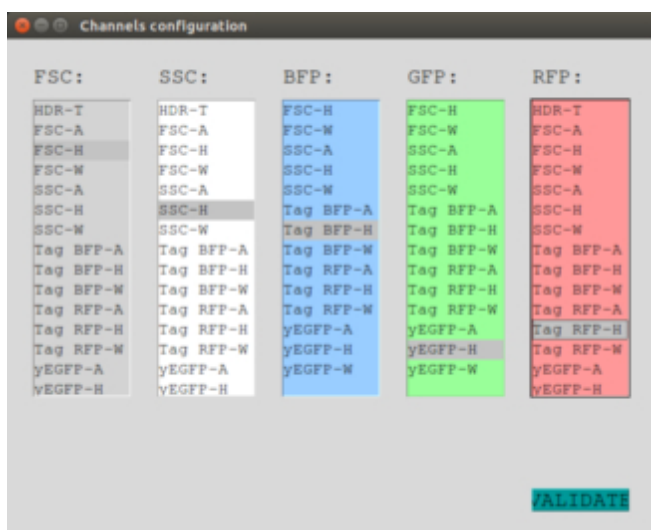


The program will identify all channels recorded in your

file. You can then attribute the correct names in the various columns. For the subsequent analysis, the column BFP corresponds to the Reporter you want to quantify. The RFP and the GFP columns correspond to the BD-Bait and AD-Prey fusion proteins respectively.

The first two columns are not used yet, but might be included in a future development of this program to sub-select a population of cells with uniform fsc and/or ssc.

The select channel names will be saved in the channels.config file (in the utils folder) when clicking on VALIDATE.



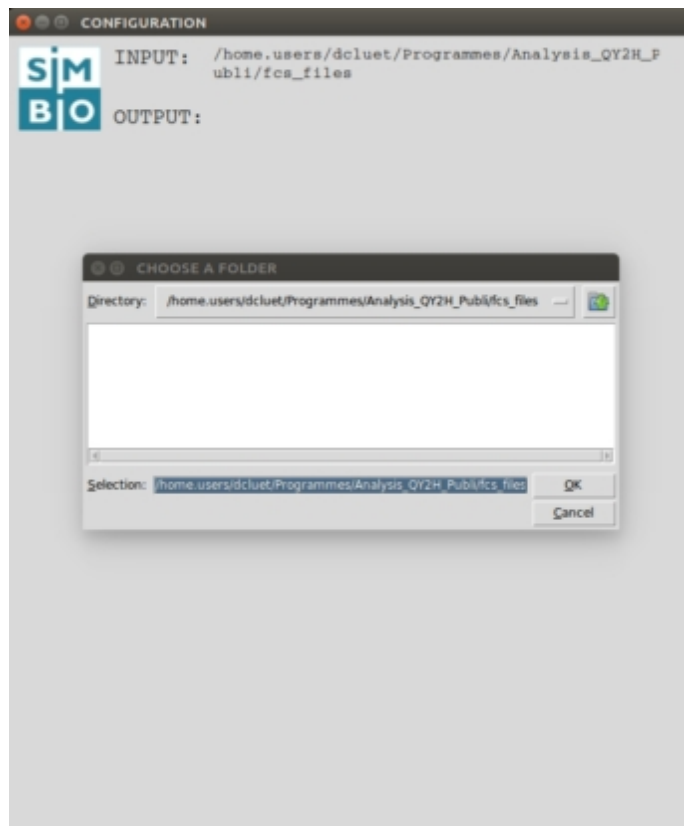
4 Perform an analysis

When clicking on `Start analysis`, the program displays the analysis configuration window. You need first to select the folder where all your files (from the same experiment) are stored.

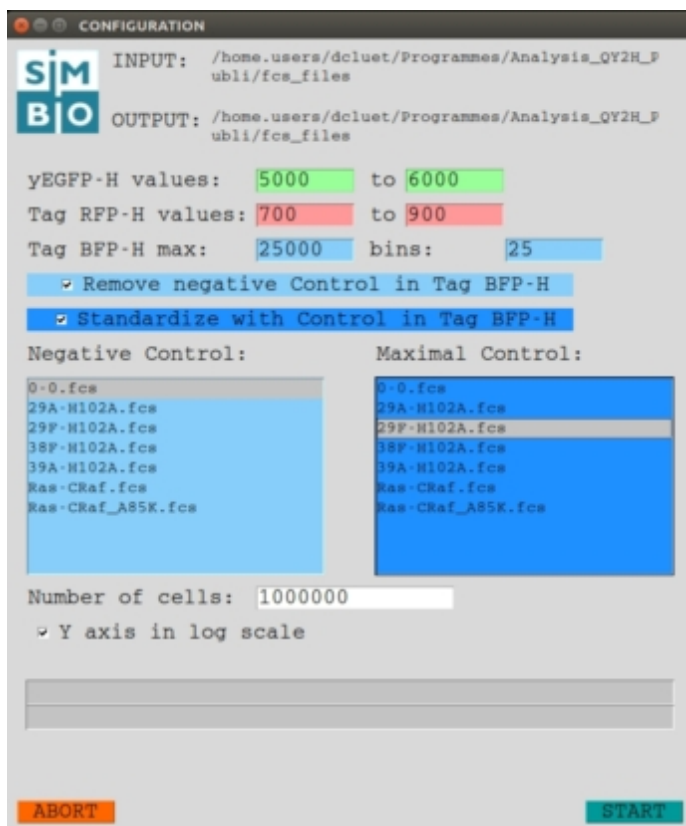
The program will automatically find all `.fcs` files present in this folder and display them in the analysis settings interface.



You need then to specify in which folder you want the output files to be generated. By default, the program is set on the input folder.



Once the path of the INPUT and OUTPUT folders are set, you have access to the analysis settings. The program will generate the Affinity ladder by taking a sub-ensemble of cells using gates in the AD-Prey GFP and BD-Bait RFP channels. By default the minimal and maximal values are set to those of the Fig. 4 (B and C) of our publication.

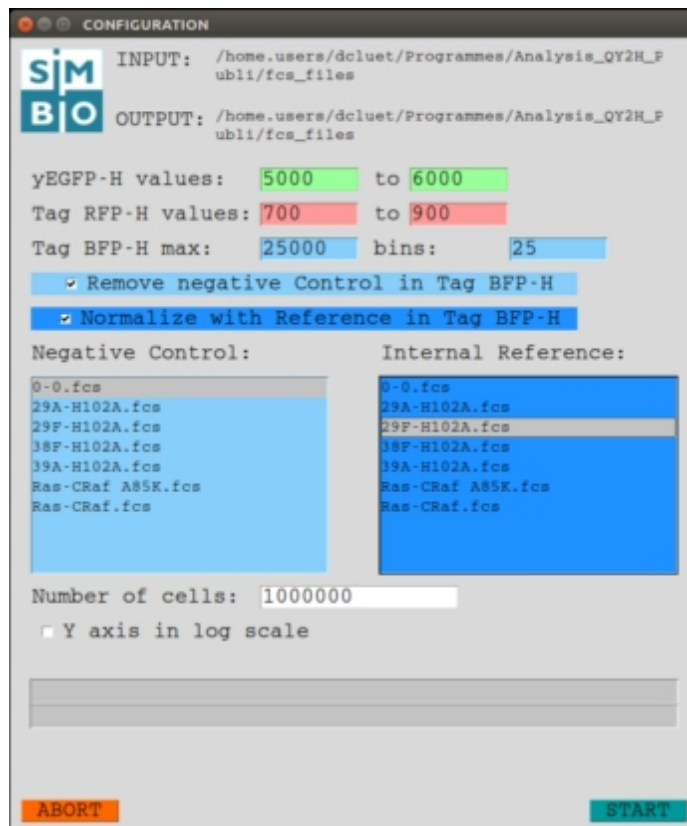


The maximum in the Reporter (BFP) channel, corresponds to the upper-limit (x axis) of the generated Cumulative mean for each sample. If the curves in the .pdf output file are not reaching a plateau, increase this value.

The value BFP bins corresponds to the number of points you want to be displayed on the final graph.

You can remove the background of the system by selecting Remove negative Control. Unchecking this option is useful to monitor the contribution of the background in your experiment. This information is helpful especially for the weakest interactors.

As the sensitivity of the system may vary from one batch of yeast to another, you can 'normalize' (to 100) the BFP signal using an Internal Reference. This will allow you to better compare various experiments. We recommend to use the strongest interaction as Internal Reference.

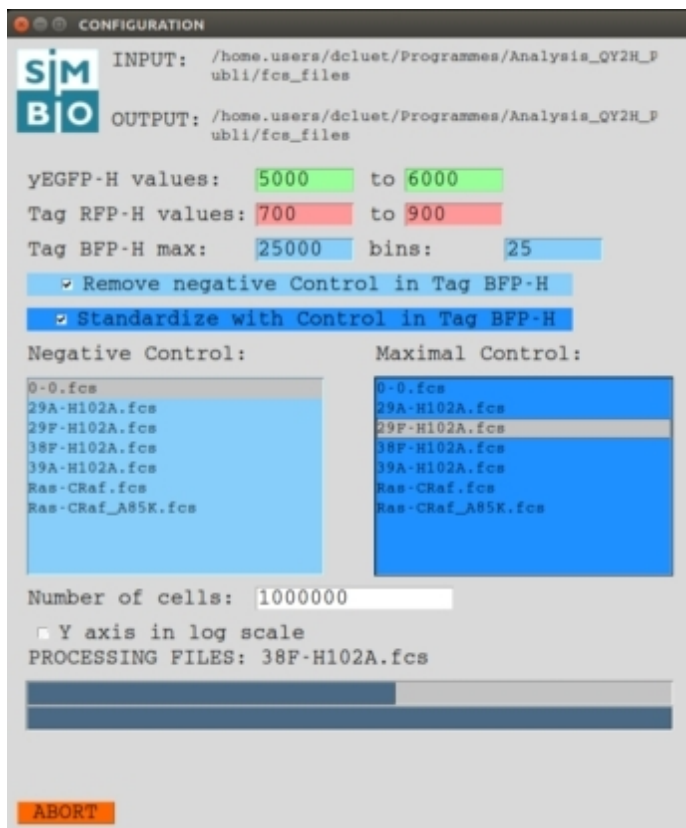


You need to specify which sample file corresponds to your negative control and Internal reference, even if no background subtraction or normalization are applied. Typically, the negative control corresponds to a qY2H experiment performed with fluorescent empty BD-Bait and AD-Prey fusion proteins. In our work, this control is called 0-0.fcs.

The value Number of cells corresponds to the maximum number of cells to be loaded from your file before doing the dual gating in the AD-Prey GFP and BD-Bait RFP channels. **We highly recommend you to analyse at least 1 000 000 events to obtain a reliable affinity ladder.**

You have the possibility to display the Cumulative mean in log or linear scale.

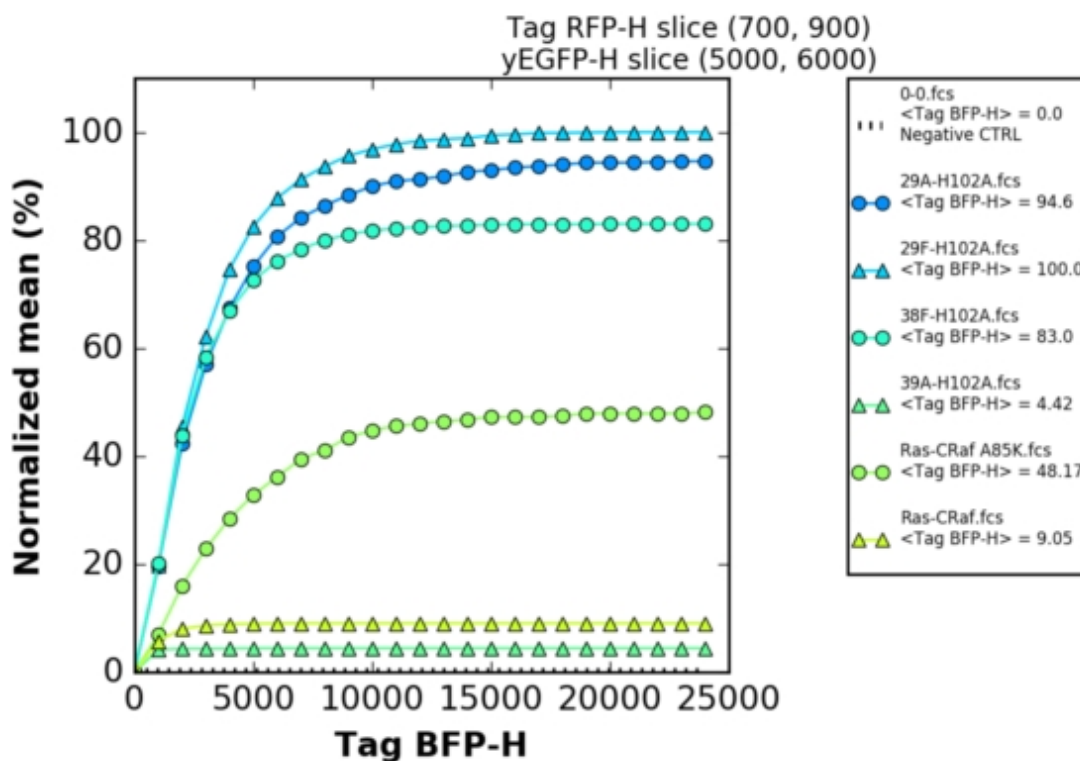
When clicking START, the program proceeds to the analysis (only if a negative control has been specified).



During the analysis the two Progress Bars inform you which file (first bar) is currently processed, and which analysis step (second bar) is performed.

Finally, the program displays the result of the analysis, with the main settings in the title. Here we present the result with the following activated options:

- **Remove negative Control**
- **Normalize with the Internal Standard**
- **Y axis in linear scale**



Click on ABORT to exit the program.

5 Output files

The program generates three files:

- A `RESULT.png` image of the graph presented at the end of the analysis
- A `.csv` table containing the mean BFP value for each sample file (after subtraction of the negative control and normalization, if selected)
- A `.pdf` report file, that encloses the qY2H affinity ladder graph.

The `.csv` and `.pdf` files have a common unique prefix based on the date and time of analysis. Moreover the data processing (*i.e.* background subtraction and/or normalisation) is explicitly indicated.

6 Example files

The flow-cytometry files of qY2H experiments can be downloaded from <http://flowrepository.org> under accession numbers:

- **FR-FCM-ZYUL** (10 millions cells)
- **FR-FCM-Z25G** (1 million cells)